I.J. Intelligent Systems and Applications, **2024, 4, 22-38**
Published Online on August 8, 2024 by MECS Press (http://www.mecs-press.org/)
DOI: 10.5815/ijisa.2024.04.02

Infrared Images Spectra Multi-class Classification Model Based on Deep Learning

Asmaa S. Abdo*
Information Systems Department, Faculty of Computers and Artificial Intelligence, University of Sadat City, Menoufia, 32897, Egypt
Scientific Research School of Egypt (SRSEG) www.egyptscience-srge.com
E-mail: asmaa.saad@fcai.usc.edu.eg
ORCID iD: https://orcid.org/0000-0001-9963-0421
*Corresponding author

Kamel K. Mohammed
Center for virus research and Studies, Al-Azhar University, Cairo, 11754, Egypt
Scientific Research School of Egypt (SRSEG) www.egyptscience-srge.com
E-mail: tawfickamel@gmail.com
ORCID iD: https://orcid.org/0000-0003-3907-8588

Rania Ahmed
Faculty of Computers and Artificial Intelligence, Modern University for Technology & Information, Cairo, Egypt
Scientific Research School of Egypt (SRSEG) www.egyptscience-srge.com
E-mail: rmohamed@cs.mti.edu.eg
ORCID iD: https://orcid.org/0009-0007-4839-8037

Heba Alshater
Department of Forensic Medicine and Clinical Toxicology, Menoufia University Hospital, Shebin El- Kom, Egypt
Scientific Research School of Egypt (SRSEG) www.egyptscience-srge.com
E-mail: heba.alshater@med.menofia.edu.eg
ORCID iD: https://orcid.org/0000-0003-2858-408X

Samar A. Aly
Department of Environmental Biotechnology, Genetic Engineering and Biotechnology Research Institute, University of Sadat City 32958, Egypt
E-mail: samar.mostafa@gebri.usc.edu.eg
ORCID iD: https://orcid.org/0000-0002-9764-865X

Ashraf Darwish
Faculty of Science, Helwan University, Cairo, Egypt
Scientific Research School of Egypt (SRSEG) www.egyptscience-srge.com
E-mail: ashraf.darwish.eg@ieee.org
ORCID iD: https://orcid.org/0000-0002-4604-1436

Aboul Ella Hassanein
Faculty of Computer and Artificial Intelligence, Cairo University, Egypt
Scientific Research School of Egypt (SRSEG) www.egyptscience-srge.com
E-mail: aboitcairo@cu.edu.eg
ORCID iD: https://orcid.org/0000-0002-9989-6681

Received: 05 April 2024; Revised: 24 May 2024; Accepted: 17 June 2024; Published: 08 August 2024

Abstract: The classification of Fourier Transform Infrared spectra images is crucial in chemometrics. This paper proposes an efficient model based on deep learning approaches for enhancement and classification of the Fourier Transform Infrared Spectra (FTIR) images. The proposed model integrates three deep learning models including ResNet101, EfficientNetB0, and Wavelet Scattering transform (WST) to extract several features from FTIR. Then the

obtained features were fused in conjunction with standard statistical feature extraction. It followed by a subsequent classification phase that employs a Convolutional Neural Network (CNN) architecture, which demonstrates high accuracy in classifying the infrared spectra images into six different classes of ligands and their metal complexes. During the training phase, the network's weights are iteratively updated using the Adam optimization algorithm. This model addresses the challenge of small and imbalanced datasets through an image oversampling process. Using random over-sampling technique, it enhances the training process and overall classification performance. The extracted features were analyzed using t-distributed Stochastic Neighbor Embedding (t-SNE) to visualize high-dimensional data in two dimensions. The results of the proposed model show high classification accuracy of 0.91%, low error rate of 0.08%, a sensitivity of 0.89% and a precision of 0.89%, false positive rate of 0.01%, F1 score of 0.89, Matthews Correlation Coefficient of 0.87 and Kappa of 0.68.

Index Terms: Fourier Transform Infrared, Artificial Intelligence, Deep Learning, Chemometric, Convolutional Neural Network.

1. Introduction

The field of chemometrics has long relied on the integration of artificial intelligence (AI) to combine knowledge and capabilities in both chemical and analytical intelligence to predict chemical properties [1]. The state of the art for predicting chemical properties has improved because of development in deep neural networks (DNNs). Several property predictions have shown increased in computational accuracy and speed, ranging from atomizing energies to protein-ligand binding affinities [2]. Vibrational spectroscopy techniques are commonly employed in polymer analysis and extensively utilized for the purpose of identifying unknown materials or characterizing their chemical compositions the most widely employed one is FTIR spectroscopies [3]. For detecting the absorption of infrared light and providing a high-quality spectrum, spectroscopic methods like FTIR spectroscopy is often used by chemists to determine the chemical composition of a material. FTIR spectroscopy technique displays the infrared region of the electromagnetic spectrum, where molecules' bonds commonly oscillate at frequencies between 4000 and 400 cm^{-1}. FTIR spectroscopy spectra is regarded as very difficult datasets that are used to analyze the chemical composition of a material by measuring the infrared light absorption and producing a high-quality spectrum. It is utilized in a variety of applications, including advancing enzymatic reactions, enzymatic assays, identifying various molecular forms of many compounds, characterization of complex materials and their dynamics to speed up the design of new materials [3]. It also shows the molecular structure and composition of materials. Additionally, it is used in the fields of forensic investigation, food and beverage production, environmental monitoring and medicines. It creates a distinctive spectral fingerprint to recognize and describe different chemical substances. FTIR method provides more scans or spectral accumulations per spectrum, which has a significant impact on spectral quality. Thus, it improves numerous levels of the signal-to-noise ratio (SNR) and various baseline distortions, or interferences that impair spectral quality [4]. Besides, the necessary spectral information is often unclear and unevenly dispersed throughout the whole spectrum, making it difficult to forecast a specific attribute of compound spectra. As well as, human involvement in FTIR spectrum analysis is advantageous, but it requires a fully automated method for identifying spectra and subsequently predicting complex structures [5]. Hence, the present accessibility of diverse computer-based image processing techniques and artificial intelligence facilitated by Artificial Neural Network (ANN) algorithms, designed to forecast FTIR spectroscopy outcomes using high-performance computers, is now within reach at a reasonable expense. This achievement was previously deemed unattainable merely a decade ago [6]. Significant advancements in deep learning networks can be achieved by utilizing CNN. It has the capability to extract salient features from image sources, mirroring the human brain's ability to interpret visual objects through feed-forward data processing. This approach surpasses the performance of traditional ANN techniques when dealing with two-dimensional image data, allowing for the iterative creation of distinct feature maps.

In contemporary times, the analysis of images and signals has become increasingly significant due to the valuable information they encapsulate. This information can be found in each of the spatial and frequency domains, particularly with the advent regarding advanced spatial frequency domain imaging technologies. Hence, it has become imperative in the direction of concurrently assessing features from both domains that have the potential to enhance the representation of image elements [7]. CNN employs spatial-based analysis in its initial layers and as it progresses deeper into its architecture, the learnt filters generate convoluted features that exhibit spatial invariance [8]. To assure the representational capacity of complex features, it is necessary to incorporate further information derived from the spatial frequency domain of the image. The wavelet transformation is a method used in spatial-frequency domain analysis. It involves representing signals as brief oscillations, which allows for compression and decompression with scaling capabilities. This technique is particularly useful for capturing gradually changing signals that indicate sudden alterations in images. Additionally, wavelet transform enables multi-resolution analysis of both spatial and frequency domains [9]. The image can provide relevant information by capturing energy sub-bands that align with the desired information scale. This cannot be achieved through a separate analysis in the spatial frequency domain. The application

of wavelet transforms in image processing are diverse, encompassing tasks such as image denoising and the representation of image features for not medical and medical signal analysis. Cardiac monitoring [10], earthquake detection [11], wireless application systems [12] and climate analysis [13] are a few examples of these applications. By incorporating wavelet coefficients, the existing CNN designs can benefit from the advantages of both domain analyses, resulting in improved performance. This is achieved by introducing a more distinct set of characteristics to deal with [14]. Nevertheless, while wavelet transform is a valuable tool for signal and image processing, its direct application to images can result in notable disadvantages. These include sensitivity to shifts, limited directionality, and the absence of phase information [15]. These shortcomings have a significant impact on the representation of the image's frequency features that can be used. To mitigate this issue, the wavelet scattering technique, as proposed by [16], employs a sequence of scattering orders through the convolution of wavelet transforms with lowpass filters. This process facilitates temporal average, thereby introducing invariance to time-shifting. Consequently, the wavelet Scattering method enhances insensitivity to phase shifts by stabilizing against time-warp deformations and translations. The utilization of scattering transform coefficients can be employed for the development of resilient image classification models, as translations and tiny visual deformations have no impact on class labels. The spatial-frequency domains of images offer a means of analyzing images that is sensitive to small changes in intensity caused by variations in texture. In the field of chemometrics, it is anticipated that WS coefficients will serve as effective descriptors for characterizing the chemical composition of textures [17].

This paper proposed a multi-classification model with very limited number of images. This is achieved through the extraction of significant textural features from the image, which are subsequently combined through automated learned features derived from the CNN architecture. The un-equal distribution of input images in the dataset, particularly for classes with smaller sample sizes, is a result of inadequate training data. For the limited number of images, we have implemented an over sampling procedure to solve the imbalance of the data images over the classes. The main contribution of this paper is summarized as follow.

- The spatial and frequency-based analysis via the WST network, along by high-level sparse demonstration via CNN network, to features fusion.
- Applies image oversample process to solve the limitation of the number of input data images over the classes
- Classification of FTIR spectra images utilizing a blend of multiple textural feature

The remaining sections of this paper are structured as follows. Section 2 reviews the related work. Section 3 presents material and methods. Section 4 presents the proposed model. Section 5 describes the obtained experimental results. Finally, Section 6 concludes the key findings of this paper.

2. Related Works

The FTIR spectroscopy is still a crucial analytical instrument for the identification and characterization of chemical compounds. Numerous chemical industries, including petrochemicals and pharmaceuticals have found use for this approach. However, spectral predictions are complicated, particularly in the 500–1500 cm^{-1} fingerprint range. Chemical compounds can be recognized based on various FTIR characteristics, including spectral peak position, absorption intensity distribution and peak shape. This analytical approach has several advantages, such as non-destructiveness and the absence of fluorescence interference. In conjunction with deep learning algorithms [18]. FTIR spectroscopy was employed to swiftly identify and categorize several varieties of chemical compositions. Recent research has shown the utility of FTIR in several domains, including the analysis of food and microplastics. These studies have focused on employing FTIR to ascertain the chemical composition of materials found in food and microplastics, as evidenced by the existing association of literature.

Chen et al. [19] introduced an adaptive estimator utilizing the k-nearest neighbors (KNN) approach to differentiate between four distinct types of microplastics, achieving a commendable accuracy rate of 97%. Henrique de Medeiros Back et al. utilized support vector machine classifier (SVC) to classify the Kedzierski FTIR data into 14 distinct types of microplastics. The classification achieved an accuracy rate of 94% [20].

In their study, Yan et al. [21] employed a combination of various machine learning methods, including partial least squares judgment analysis, random forest and artificial neural network, to classify the Kedzierski dataset. This approach yielded a classification accuracy of 91.74%. CNN has demonstrated their efficacy in various domains, including target detection, face recognition, image classification and other related areas. When compared to other techniques, CNN exhibits superior generalization abilities in the field of image processing.

In recent years, there has been a growing trend in converting one-dimensional spectra into two-dimensional images, followed by the construction of classification models using CNN network. Zhang et al. [22] successfully transformed one-dimensional near infrared spectroscopy (NIRS) data into two-dimensional spectral pictures. Additionally, they introduced a novel identification approach for tobacco NIRS using CNN. The classification accuracy achieved a notable improvement of 93.05%, surpassing the performance of conventional approaches. McGill et al. [23] utilized the training approach of the Chemprop-IR prediction model involved utilizing a selection of chemicals obtained from PubChem to generate a total of 85,232 computed spectra. These computed spectra are then utilized to pretrain a model. Subsequently,

the parameters within the feedforward neural network are refined using 56,955 experimental spectra.

The utilization of image fusion in the development of classification models is advantageous due to its ability to effectively leverage the features present in FTIR spectrum images. This is particularly valuable as these images encompass diverse spatial information. In recent years, CNN has emerged as a significant catalyst in shaping the advancement of image fusion. In contrast to conventional image fusion algorithms, CNN-based image fusion algorithms have the capability to extract a greater amount of feature information, resulting in enhanced image quality. Moreover, these algorithms are versatile and may be applied to various image fusion applications. Chen et al. [24] employed CNN network to analyze time series data, visual imaging, language processing, face recognition and age prediction NIR spectral data with accuracy 91.4%. Jung H et al. [25] developed a deep image fusion network (DIF-Net) utilizing CNN for the purpose of fusing multiple types of images.

Previous research presented by Ailing Tan et al. [26] has integrated wavelet transform into the architecture of CNN. However, this approach introduces additional computational time as the CNN needs to learn filter weightage from the images and perform wavelet transform tasks simultaneously. Moreover, it also adds complexity to the overall pipeline. In addition to the absence of phase shift information, traditional wavelet-based features have certain limitations. These features were extracted from individual images per class, unlike the wavelet scattering approach which necessitates a deep training process that establishes connections between all images' wavelets per class on its scalogram. This process involved a connected filtering process, like the weight learning process in CNN architecture. In order to tackle this issue, the present research proposes employing wavelet composition *via* wavelet scattering that is taught separately from the CNN architecture, requiring only minimum additional training time. To the best of our current understanding, there is a lack of comprehensive investigation into the utilization of WS coefficients as textural features in the classification of chemical compositions using CNN. In addition, it is crucial to construct a robust system by minimizing the number of training images and employing optimal feature selection using WS coefficients. Significant existing works regarding FTIR spectrum classification and prediction are summarized in Table 1.

Table 1. Comparison of different related work

Ref.	year	Methods	Dataset	Accuracy	Limitations
[18]	2021	Support vector regression (SVR)	The NIR spectra of 100 samples were collected using the visible and near-infrared (VIS-NIR) spectrometer, which has a spectral range of 300–1160 nm and 945 wavelengths.	97.13% to 98.82%	The dataset is small to train and test model.
[19]	2021	KNN Robust KNN model classifier.	Four different datasets of MPs samples as PE, PET, PP, PS with more than 400 spectra were applied	91.9% with KNN 97% with robust KNN model	Need to use different model where it was found that the KNN model performed not well on the samples with distortion feature,
[21]	2022	Ensemble learning based on SVM, KNN and RF	-Imbalanced FTIR dataset. - Kedzierski dataset containing 970 spectra. - Jung dataset containing 798 spectra	94.19% in first dataset 94.% in second dataset	Comparing KNN with SVM, manipulation has a greater impact on SVM, whereas dataset imbalance has a greater impact on KNN (SVM performs better than KNN in small sample sizes).
[23]	2021	Chemprop-IR based on DL and ensembling model	Four external data sources (NIST, PNNL, AIST and Coblentz Society)	96.9%	Didn’t apply pre-processing on dataset
[24]	2020	CNN deep learning model	The NIR spectral data	91.4%	Need to enhance accuracy

3. Material and Methods

3.1. FTIR Instrument Measurements

The samples were assessed using attenuated total reflection (ATR)-FTIR spectroscopy with a Bruker Tensor 27 System (Bruker Optics GmbH) with a diamond platinum ATR-unit (Bruker Optics GmbH) in order to establish a generic spectrum database. The absorbance spectra were captured using 32 scans at a resolution of 4 cm−1, covering the range of 4000 to 400 cm^{-1}. Every measurement was carried out three times. A transmission mode measurement was also performed on the chosen materials using a μ FTIR microscope.

3.2. Preparation of Ligands and Metal Complexes

A total of 211 FTIR spectral images, representing three derivatives of organic compounds and their metal complexes. There were synthesized by combining ethanolic solutions of different metal salts (MX_2) with ethanolic solutions of ligands. These samples were collected by the co-authors of this paper (Dr. Samar and Dr. Heba) and are detailed in previous publications [27-31] as shown in Table 2.

Table 2. Total FTIR classes and sample of them

Ref	Year	FTIR Class Name	Number of Class Images
[27]	2019	Class1 Thiosemicarbazide ligand	6
[28]	2021	Class 2 Metal complexes of Thiosemicarbazide	55
[29]	2018	Class 3 Hydrazone	9
[31]	2021	Class 4 Antipyrine	14
[30]	2020	Class 5 Metal complexes of Hydrazone	61
[32]	2022	Class 6 Metal complexes of antipyrine	66

3.3. Deep Learning Models

The deep learning models employed include ResNet101, EfficientNetB0 and Wavelet scattering transform.

- ResNet101: It is an abbreviation for Residual Network. It is a CNN with 101 layers, which is specific type of ResNet that has their specific residual block [33]. Instead of attempting to extract certain features, residual learning extracts the residual. It has been demonstrated that training using these designs is more effective than training with common deep CNN [34, 35]. The equation simplified representation of this model as shown in equation 1.

$$y = Fx, w1w2|w3 + x \tag{1}$$

where *x* is the input feature map to the block, *w1*, *w2*, *w3* are the weights of the convolutions, respectively, *F* is the composite function of these three convolutions with associated activation and batch normalization, which the network will learn, y is the output feature map of the block.

- EfficientNetB0 is a mobile network that employs a multi-objective network search to improve accuracy. It depends on MobileNetv2. Also, employs a scaling procedure that consistently balances the width, depth, and picture size dimensions utilizing an additive coefficient (α, β, and γ) [36, 37].
- Wavelet scattering transform network depicts its idea from deep neural networks, due to their shared characteristics. Wavelets play a role in this process by providing a sparse representation of the input signal. They achieve this by filtering out unnecessary information while retaining important details through a process of averaging [38]. Formally, the scattering transform can be described with the equations as in [39]. The equations below indicate the calculation of zero order, first order, and second order dispersion coefficients.

  - Zero order:

$$S_0 x(t) = x * \varphi(t) \tag{2}$$

where *x* is the input signal, $*$ denotes convolution, and ϕ is a low pass filter.

- First order:

$$S_1 x(t, \lambda_1) = |x * \psi\lambda_1| * \phi(t) \tag{3}$$

where $\psi\lambda_1$ is a wavelet at scale λ_1.

- Second order:

$$S_2 x(t, \lambda_1, \lambda_1) = ||x * \psi\lambda_1| * \psi * \phi(t) \tag{4}$$

3.4. Traditional Image Analysis Techniques for Feature Extraction

The research also includes a set of four features are utilized such as Intensity Histogram, Gray-Level Co-occurrence Matrix (GLCM), Gray Level Run Length Matrix (GLRLM) and Invariant Moments. The objective is to extract high-level and distinctive features suitable for classification tasks, as explained in the following details.

- Intensity Histogram: An intensity histogram represents the distribution of pixel intensities (gray levels) in an image. It captures the underlying intensity characteristics. The histogram provides insights about the contrast, brightness, and intensity distribution of an image [40]. The general formulation of it can be defined in equation 5 as follows:

$$P_i = \frac{n_i}{N} \tag{5}$$

where Pi is the probability of an intensity level i, n_i represents the number of pixels that have an intensity level of i, N represents the total number of pixels present in the image.

- The GLCM feature is employed to calculate various textural features of an image. These extracted features include contrast, correlation, homogeneity, and several others. It's a powerful tool for texture analysis [41].
- The GLRLM feature captures the distribution of runs (consecutive pixels) of specific gray levels and lengths in an image. It enables the computation of various texture features, including short run emphasis, long run emphasis, run length non-uniformity, gray level non-uniformity and more. GLRLM provides another perspective on the texture of an image [42].
- Invariant Moments: are a collection of seven moments that are invariant to image transformations, such as translation, rotation, and scaling. These moments are particularly valuable in recognizing or describing a shape in an image, regardless of its orientation, size, or position [43].

4. The Proposed Infrared Images Spectra Multi-class Classification Model

This section discusses in detail the proposed classification model for FTIR spectra images. The architecture of the proposed model is shown in Fig.1. The proposed model involves three phases to enhance the model ability to accurately differentiate between six classes of spectral data.

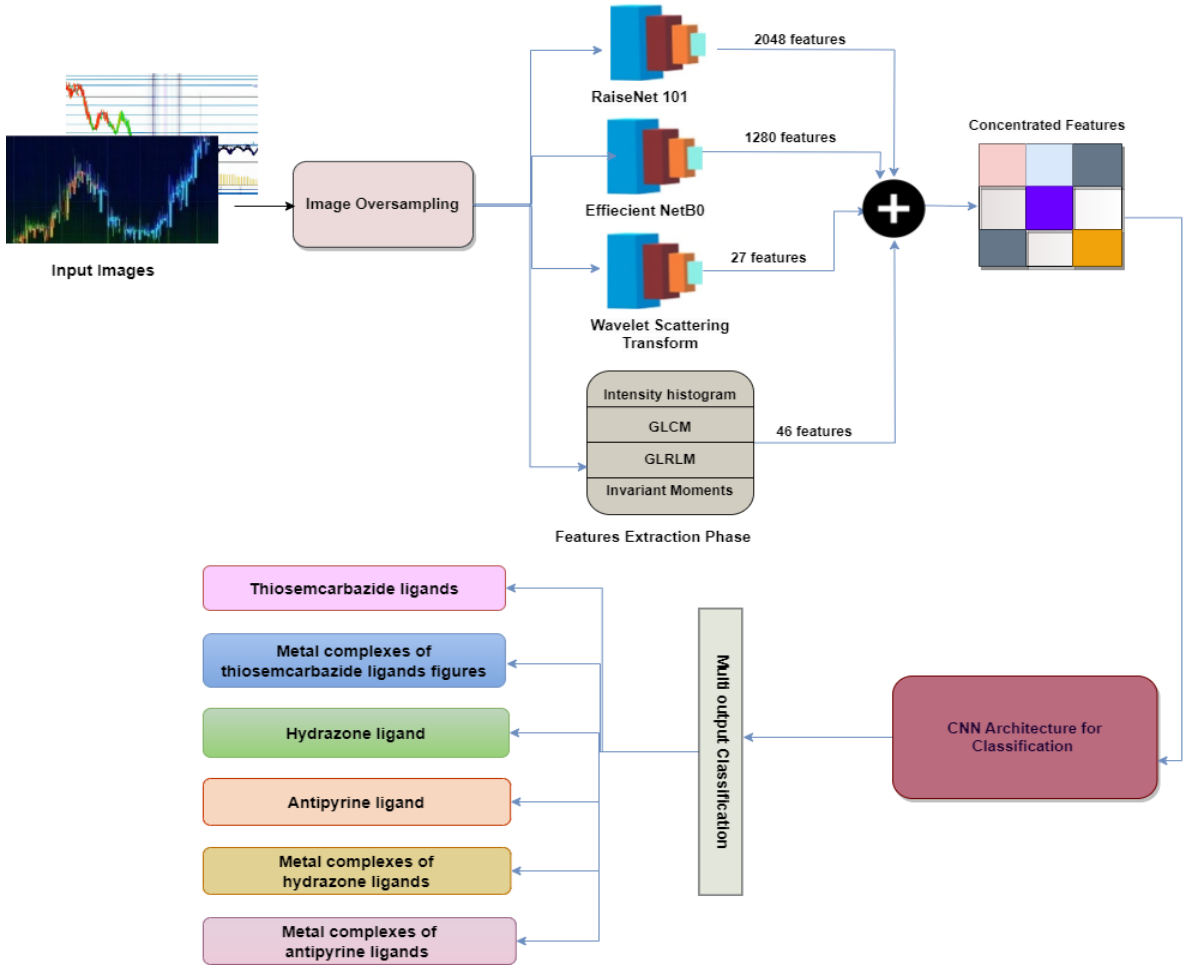

Fig.1. The proposed classification model for FTIR spectra data

4.1. Phase 1: Image Oversampling

The initial phase addresses the common issue of class imbalance in the dataset. Due to the imbalanced nature of input FTIR spectra images dataset and limited training data, especially for the smaller number classes. In this phase, the model applies an image oversampling process. This involves randomly iterating the minority classes to equalize them with the majority classes, by generating additional synthetic images for the less-represented samples. The random

oversampling technique balances the representation of minority classes before feature extraction phase as indicated in [44].

4.2. Phase 2: Feature Extraction

The second phase involves processing the FTIR spectra image data through multiple deep learning models as well as traditional image analysis techniques. The deep learning models used include ResNet101, EfficientNetB0, and Wavelet Scattering Transform. ResNet101 is a CNN with 101 layers that extracts 2048 distinct features from each image. EfficientNetB0 is a mobile network that extracts 1280 features. The Wavelet Scattering Transform extracts 27 features by filtering out unnecessary information and retaining important details through averaging. Traditional image analysis techniques contribute an additional 46 features. These techniques include the Intensity Histogram, which captures 6 features, the GLCM with 22 features, the GLRLM with 11 features, and Invariant Moments with 7 features. The features extracted from both deep learning models and traditional techniques result in a concentrated set of 6000 features for each image.

4.3. Phase 3: CNN Architecture-based Classification

After feature extraction, the third phase involves using the CNN architecture for classification. The concentrated features output is passed to the CNN architecture for classification. As depicted in Fig. 2, the CNN architecture includes the following sequence of layers:

- Feature Input Layer: This layer initializes the input size, taking the features as input and normalizing them using z-score normalization. This layer is responsible for preparing the input data for further processing. Let's represent the input vector as X is which has a size of "$Numfeatures$".

$$X = [x_1, x_2, \dots, x_{Numfeatures}] \tag{6}$$

- Fully connected layers: These layers are responsible for learning complex patterns in the input features. Each neuron in these layers is connected to all neurons in the previous layer, enabling them to learn from all features simultaneously. This layer contains 500 neurons.

$$A_1 = W_1 \times X + b_1 \tag{7}$$

Where W_1 is a 500× $Numfeatures$ weight matrix. Each row of this matrix corresponds to a neuron in a neural network, and each column corresponds to a weight for each input feature, b_1 is a bias vector of size 500 ×1, A_1 is the output vector of size 500×1 matrix before applying the activation function.

- Dropout layers: Each fully connected layer is combined with dropout layers for regularization and batch normalization layers to stabilize and speed up the training. A dropout layer with a dropout rate of 0.5 randomly deactivates half of the neurons in the previous layer during training, helping to prevent overfitting.

- The batch normalization layers: These layers normalize the activations of the previous layer and reducing the internal covariate shift during training. Batch normalization is performed in smaller batches rather than using the entire dataset. It is accomplished by fixing the means μ_B and variance σ_B^2 of each input layer during the normalization step as shown in two equations below.

$$\mu_B = \frac{1}{m}\sum_{i=1}^{m} x_i \tag{8}$$

$$\sigma_B^2 = \frac{1}{m}\sum_{i=1}^{m}(x_i - \mu_B)^2 \tag{9}$$

where *B* denotes the mini batch of the size *m* of the whole training set.

- The ReLU layers: The rectified linear unit (ReLU) is an activation function introducing non-linearity. The adoption of ReLU prevents the neural network's computation from growing exponentially. It also avoids the vanishing gradient problem. The ReLU layer returns 0 if any negative input is received; even though the function returns the positive value it receives for *x* as shown in equation 10 below.

$$R(x) = \begin{cases} 0 & for\ x < 0 \\ x & for\ x \geq 0 \end{cases} \tag{10}$$

- The SoftMax Layer: is used in multi-class classification task. It is typically applied to the output of the last fully connected layer of a CNN architecture. It transforms the raw output values, represented as a vector of logits $\vec{z}$, into probability scores for each of the six classes. The probability of a data point belonging to each

individual class is provided by the SoftMax Activation function as shown in equation 11 below. These probabilities are the model predictions for each of the six classes.

$$\sigma(\overrightarrow{z})_i = \frac{e^{z_i}}{\sum_{j=1}^{k} e^{z_j}} \tag{11}$$

where $\vec{z}$ is the input vector, e^{z_i} is the exponential function for input vector, K is the number of classes, e^{z_j} is the exponential function for output vector.

- Classification Layer: This layer produces the final classification results in a multi-output classification task. It classifies the input into one of six distinct classes:
  - Thiosemcarbazide ligands
  - Metal complexes of thiosemcarbazide ligands figures
  - Hydrazone ligand
  - Antipyrine ligand
  - Metal complexes of hydrazone ligands
  - Metal complexes of antipyrine ligands

The proposed image classification network combines traditional feature extraction methods with a robust CNN architecture to achieve high accuracy in classifying images into specific chemical ligand classes.

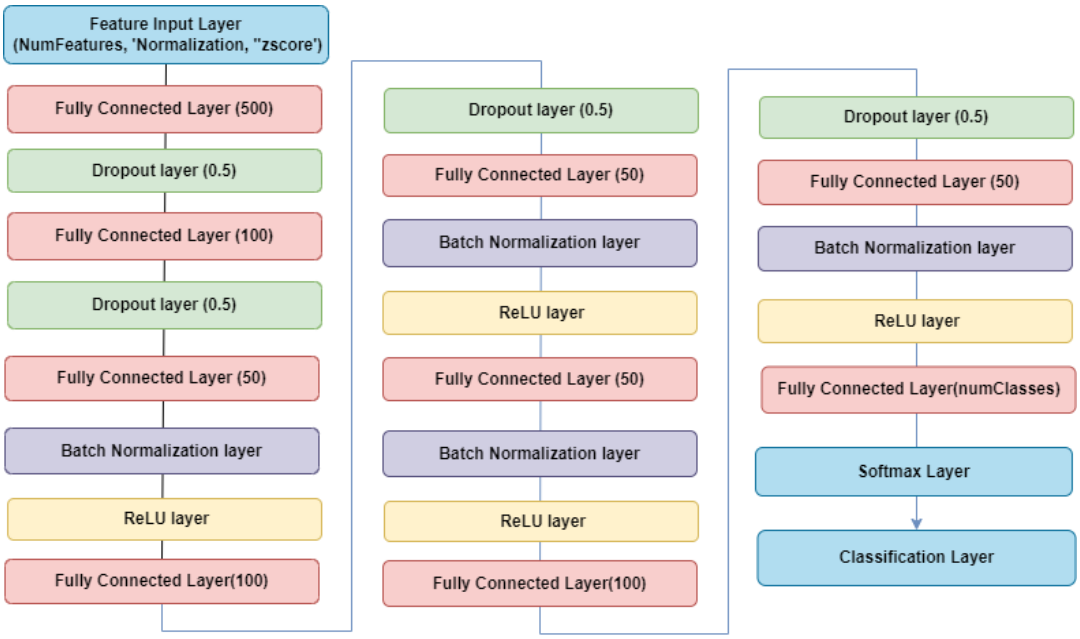

Fig.2. The proposed CNN architecture

The CNN architecture was trained using the Adam optimizer, which iteratively updates the network weights during training [45]. As shown in Table 3, several parameters were employed to train the model. The initial learning rate was set to 0.001, indicating the step size at which the weights are adjusted. This learning rate was reduced by a factor of 0.5 every 5 epochs. The training process reach over 200 epochs. The neural network training process involved using a batch size of 16, which determined the number of samples utilized in each epoch.

Table 3. Parameters value utilized by adam optimizer

Evaluation Measures	**Testing Results**
Accuracy	0.9111
Error Rate	0.0889
Sensitivity	0.8963
Precision	0.8963
False Positive Rate	0.0176
Accuracy	0.9111

5. Experimental Results and Evaluations

The results of the proposed model and evaluation metrics of the experiments are presented in this section. The experiments were conducted using a GPU optimized for MATLAB R2022b software. All experimental tasks were managed by the GPU on a computer equipped with a core i7 processor and 16 GB of RAM.

5.1. Dataset Preparation and Oversampling

Initially, after collecting the dataset, the FTIR spectra images were resized to ensure uniformity across all image files. To address the class imbalance in the image data, an oversampling process was employed. The initial dataset consisted of 211 image files with an uneven number of samples across different classes. To achieve a balanced distribution, additional copies of image files were created within the underrepresented classes through oversampling. This increased the total number of image files to 294, with each class containing 49 samples. The before and after states of the oversampling process are illustrated in Fig.3 below.

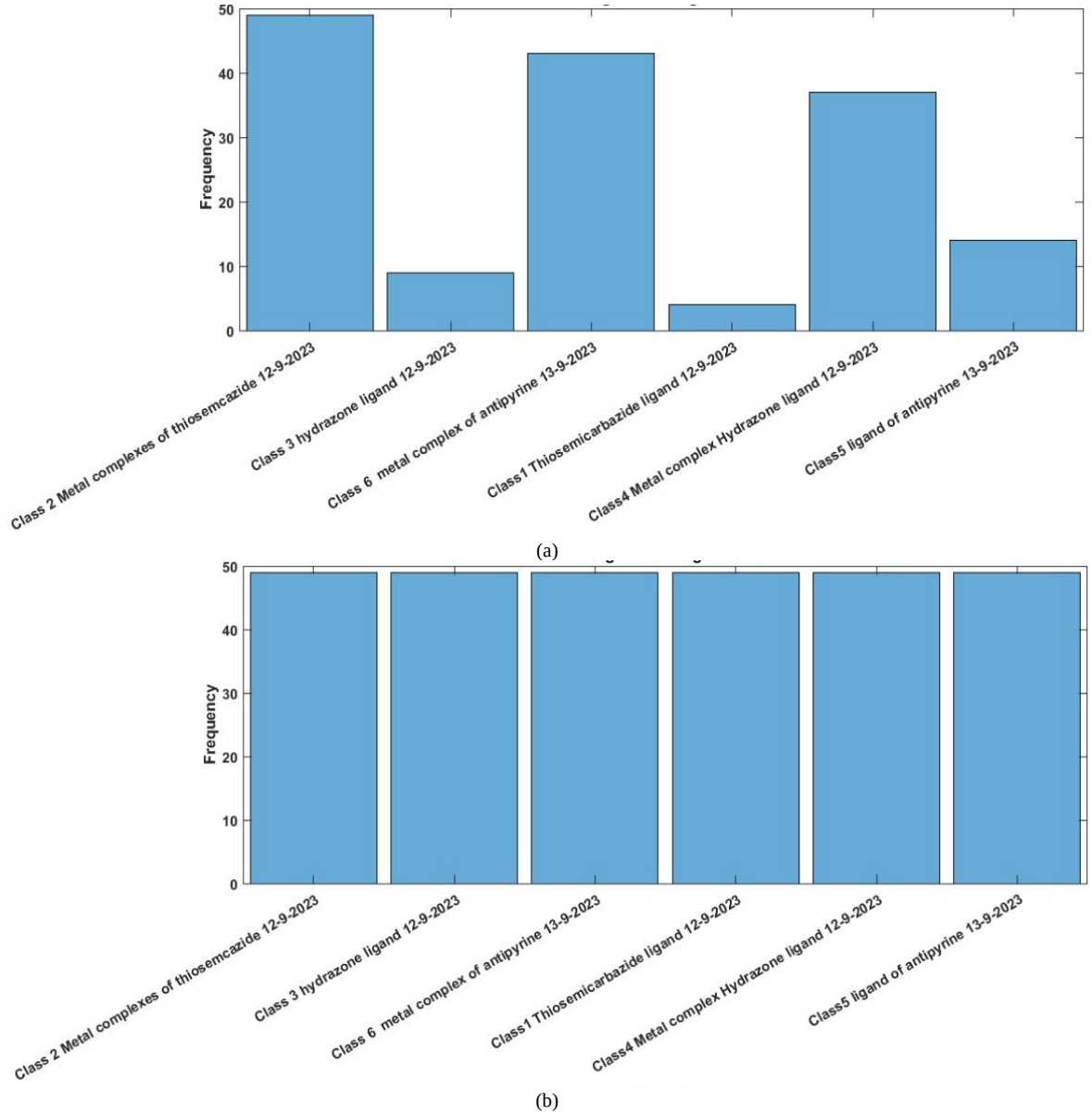

Fig.3. The oversampling process. (a) Before oversampling. (b) After oversampling

5.2. Classification Results

Fig.4 shows the evaluation of accuracy results for six classes using a confusion matrix. The confusion matrix shows the performance of a multi-output classification provides a visual representation for each class. The model achieved an overall accuracy of 91.11%, indicating well performance. Also, all classes have a true positive rate of 100%, indicating that the model is able to accurately classify images of these classes.

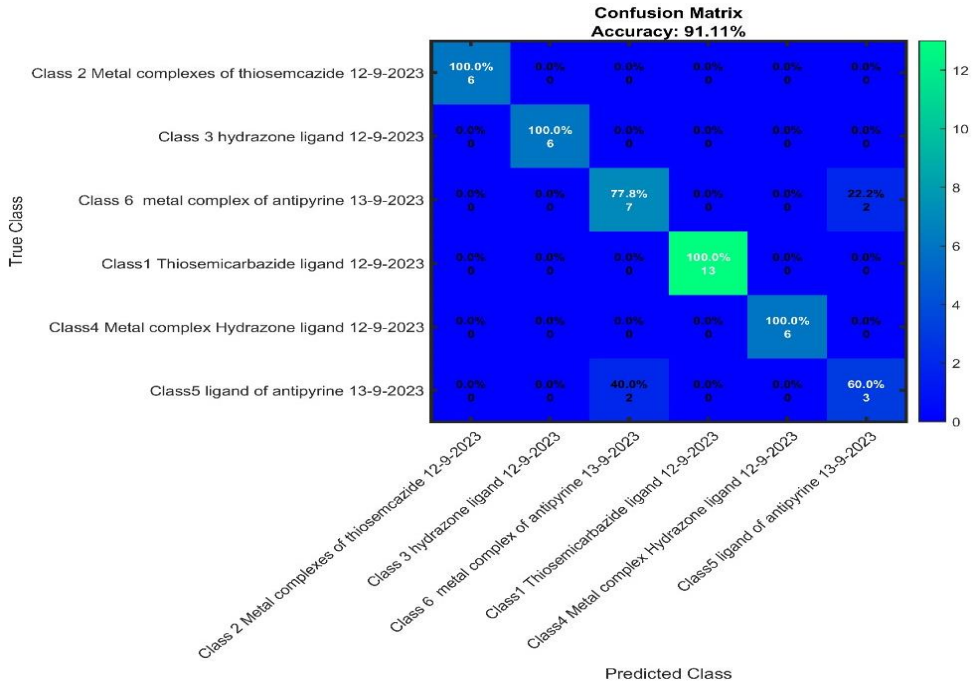

Fig.4. The confusion matrix of six classes in testing accuracy results

5.3. Evaluation Metrics

Table 4 summarizes the evaluation results of the proposed model in testing results. Several metrics are employed to measure the performance such as accuracy, Error, Sensitivity, precision, False Positive Rate, F1_score, F-Measure, Matthews Correlation Coefficient and Kappa. The definitions of the metrics are as follows:

$$Accuracy = \frac{TP+TN}{TP+\mathrm{TN}+FN+FP} \tag{12}$$

$$Error\_Rate = \frac{FP+FN}{N} \tag{13}$$

$$Sensitivity = \frac{TP}{TP+FN} \tag{14}$$

$$Precision = \frac{TP}{TP+FP} \tag{15}$$

$$False\ Positive\ Rate = \frac{FP}{TN+FP} \tag{16}$$

$$F1\_Score = \frac{2TP}{2TP+FP+FN} \tag{17}$$

$$Matthews\ Correlation\ Coefficient = \frac{TP\times TN-FP\times FN}{\sqrt{(TP+FP)(TP+FN)(TN+FP)(TN+FN)}} \tag{18}$$

$$Kappa = \frac{p_r-p_h}{1-p_r} \tag{19}$$

where TP is the True Positive, FP is the False Positive, FN is the False Negative, TN is the True Negative, N is the total number of cases, p_r is the relative observed agreement among raters, p_h is the hypothetical probability of chance agreement.

The high accuracy (0.9111) indicates that the model correctly predicted outcomes in most cases. The low error rate (0.0889) shows minimal errors. High sensitivity (0.8963) and precision (0.8963) indicate effective identification of positive cases and correct positive predictions, respectively. The low false positive rate (0.0176) proposes accurate identification of negative cases. The F1 score (0.8963), Matthew's correlation coefficient (0.8787), and Kappa value (0.6800) further confirm the model's robust performance and reliable agreement between predicted and actual outcomes.

Table 4. Overall results of evaluation

Evaluation Measures	Testing Results
Accuracy	0.9111
Error Rate	0.0889
Sensitivity	0.8963
Precision	0.8963
False Positive Rate	0.0176
F1_score	0.8963
Matthews Correlation Coefficient	0.8787
Kappa	0.6800

5.4. Training Progress

The FTIR spectra images dataset was split into training (70%), validation (15%), and testing (15%) sets to evaluate the proposed model performance. Fig.5 shows the training accuracy versus loss curve, indicating model performance during training. Training was performed over 200 epochs each including 6 iterations and summing up to a total of 1200 iterations. The model achieved high training accuracy (0.9111), indicating effective learning of underlying patterns from data. The total training time was 46 seconds. This indicates that the model was updated frequently during training contributing to high accuracy. The validation frequency of 30 iterations allowed for regular monitoring of the model performance on unseen data, which is important for preventing overfitting.

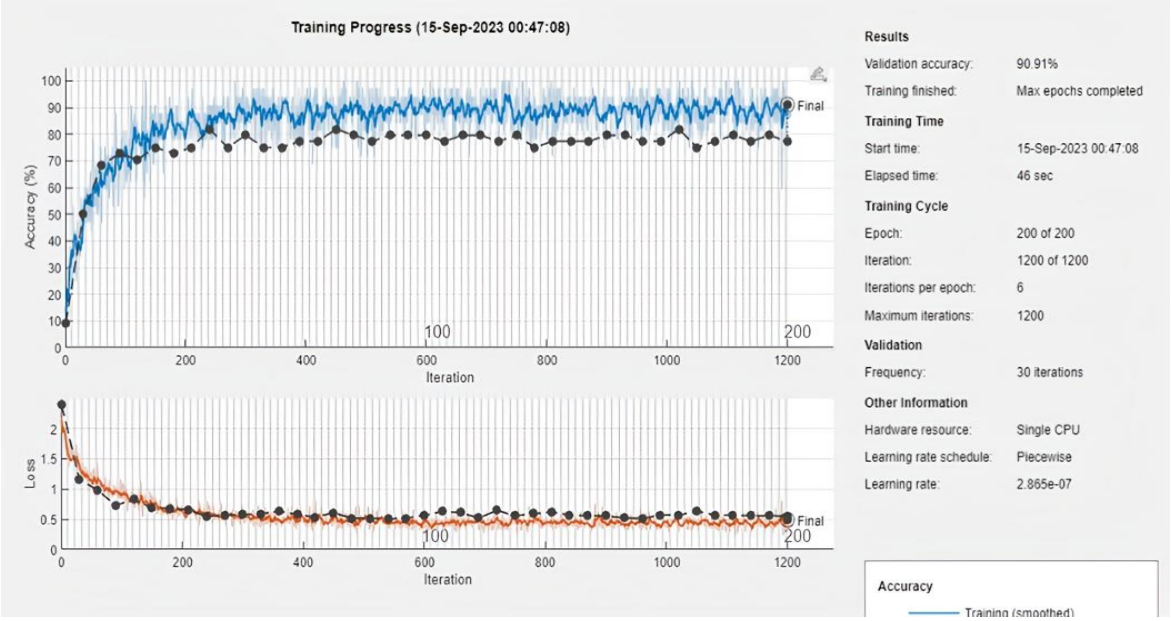

Fig.5. Training progress accuracy and loss curves for the proposed model

5.5. ROC Curve Analysis

Receiver Operating Characteristic (ROC) curve analysis was performed on the testing dataset to evaluate model performance. As displayed in Fig. 6, the x- axis represent false positive rate (1-specificity), and another y- axis is the true positive rate (sensitivity). The ROC curve illustrates the trade-off between sensitivity and specificity [46].

5.6. Histogram Visualization of Weights and Biases

Histogram visualization of Weights for FC 500 Layer provide visualization of the distribution of weights and biases in a fully connected layer with 500 neurons [47]. In Fig.7, The x- axis represents weight value and y-axis represents frequency. This can be effective for understanding the spread and range of weights within the layer, which can give insights into the learning process. Also, in Fig.8, The x- axis represents biases value and y-axis represents frequency. This help to give insights into the distribution of biases and help in understanding the behaviour of the layer.

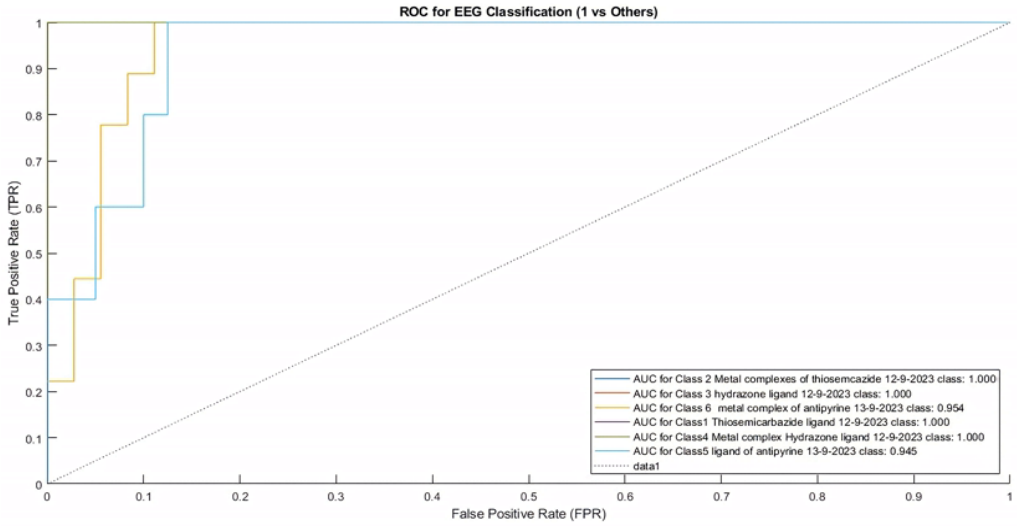

Fig.6. ROC curve for testing dataset

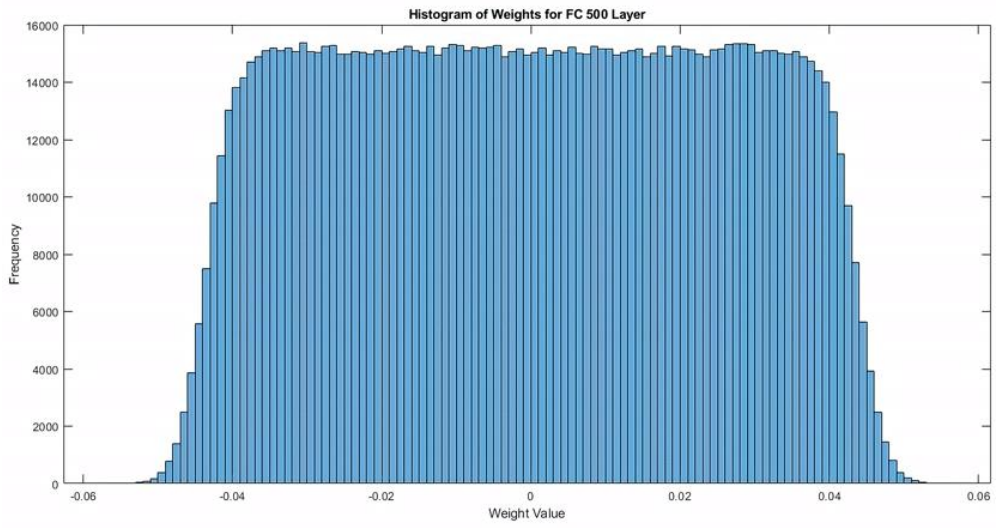

Fig.7. Histogram of weights for FC 500 layer

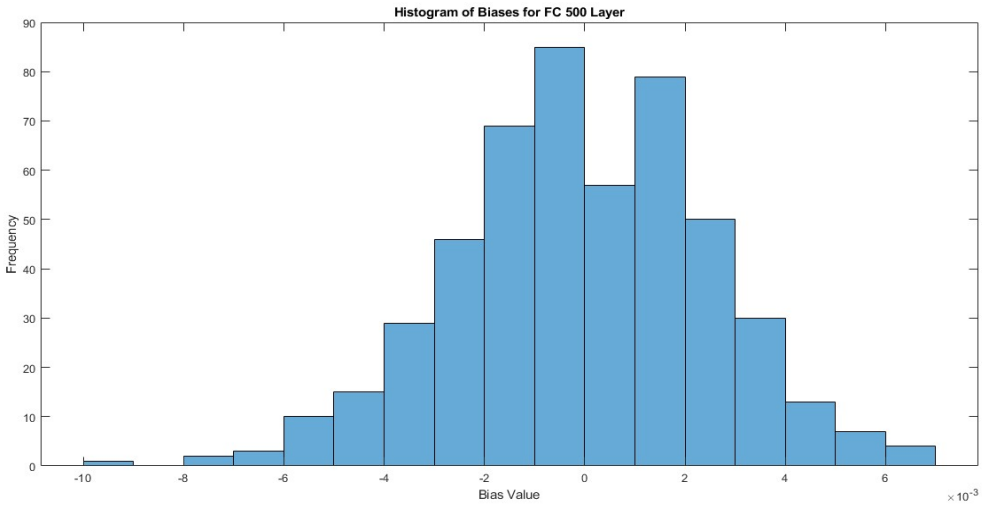

Fig.8. Histogram of biases for FC 500 layer

5.7. t-SNE Feature Analysis

The The extracted features were analyzed using t-distributed Stochastic Neighbor Embedding (t-SNE) to visualize high-dimensional data in two dimensions [48]. Fig. 9. shows the 2D t-SNE visualization of the feature space, indicating that most classes are well separated. However, the poor separation of " Class 3 - hydrazone ligand " and " Class 4 - Metal complex Hydrazone ligand ", indicating that some shared features or similarities.

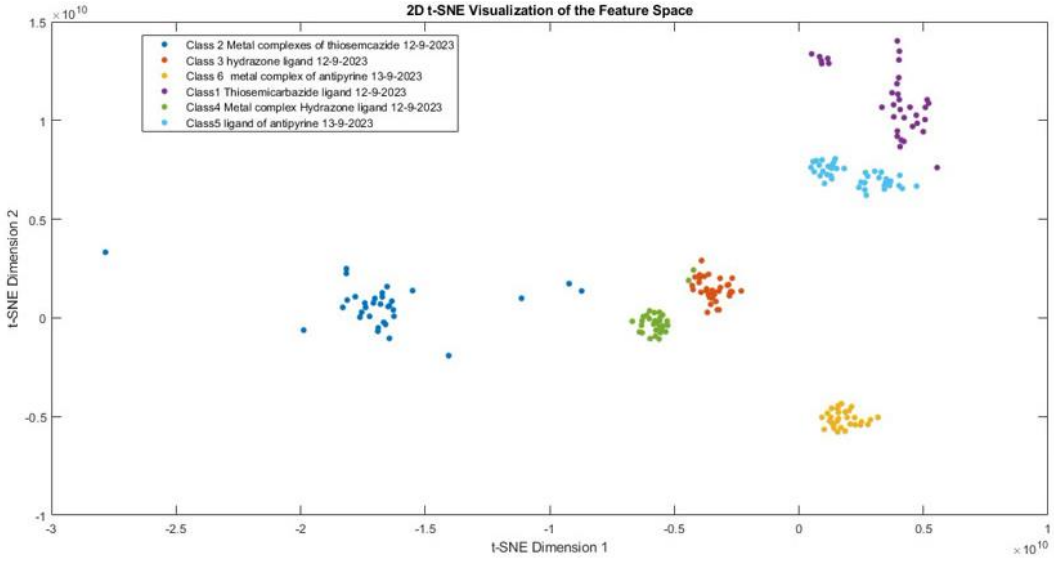

Fig.9. The 2D t-SNE visualization of the feature Space indicating relationships between classes

The discussion of the above results presented in this section is summarized in the following. The challenge of interpreting spectral data for chemical compounds is a big problem facing chemists for classification and prediction of classes. The feature extraction phase from the data simplifies the complexity. It helps increase the performance of the analysis process from FTIR spectra images dataset, com-pared to traditional methods used by chemists. In addition, the proposed classification model for FTIR spectra images in chemometrics field, effectively classifies images based on six ligand and metal complex classes. Despite the limitation of the availability of large and diverse FTIR image datasets, the proposed model demonstrates significant promise for future applications in chemometrics and other fields requiring precise chemical compound characterization.

6. Conclusion and Future Work

This paper presents an efficient model for classifying FTIR spectra images using integrated deep learning models. Combining ResNet101, EfficientNetB0, and Wavelet Scattering Transform (WST) with traditional image analysis techniques ensures the extraction of high-dimensional, distinctive features from FTIR spectra images. The CNN-based classification model successfully categorizes these images into six classes, demonstrating higher accuracy. The proposed model addresses the essential challenges of small and imbalanced datasets through an effective image oversampling technique, thus optimizing the training process. Despite the limitations of the availability of large and diverse FTIR image datasets, the proposed model shows significant promise for future applications in chemometrics and other fields requiring precise chemical compound characterization. Future research will focus on extending the model to classify additional FTIR spectroscopy images based on their chemical characteristics.

Data Availability

The dataset utilized in this research paper is available upon request.

Competing Interests

There is no conflict of interests.

References

[1] Marini F., et al., Artificial neural networks in chemometrics: history, examples and perspectives, Micro chem. J. 88 (2) (2008) 178e185.
[2] Wang, X., Ye, S., Hu, W., Sharman, E., Liu, R., Liu, Y., Luo, Y., Jiang, J.: Electric Dipole Descriptor for Machine Learning

Prediction of Catalyst Surface–Molecular Adsorbate Interactions. Journal of the American Chemical Society. 142, 7737–7743 (2020). https://doi.org/10.1021/jacs.0c01825.
[3] Everall, N. J.; Chalmers, J. M.; Griffiths, P. R. Vibrational Spectroscopy of Polymers: Principles and Practice; Wiley: Chichester, (2007).
[4] Brandt, J., Mattsson, K., Hassellöv, M.: Deep Learning for Reconstructing Low-Quality FTIR and Raman Spectra─A Case Study in Microplastic Analyses. Analytical Chemistry. 93, 16360–16368 (2021). https://doi.org/10.1021/acs.analchem.1c02618.
[5] Fine, J.A., Rajasekar, A.A., Jethava, K.P., Chopra, G.: Spectral deep learning for prediction and prospective validation of functional groups. Chem. Sci. 11, 4618–4630 (2020). https://doi.org/10.1039/C9SC06240H.
[6] Oren O., Gersh B.J., Bhatt D.L., Artificial intelligence in medical imaging: switching from radiographic pathological data to clinically meaningful endpoints, Lancet Digit. Heal. 2 (9) (2020) e486, https://doi.org/10.1016/S2589-7500(20) 30160-6.
[7] Gioux, S., Mazhar A., Cuccia D.J., Spatial frequency domain imaging in 2019: principles, applications, and perspectives, J. Biomed. Opt. 24 (7) (2019) 1–18, https://doi.org/10.1117/1.JBO.24.7.071613.
[8] Sarvamangala, D.R., Kulkarni, R. V: Convolutional neural networks in medical image understanding: a survey. Evolutionary Intelligence. 15, 1–22 (2022). https://doi.org/10.1007/s12065-020-00540-3.
[9] Akujuobi, Cajetan M. Wavelets and wavelet transform systems and their applications. Berlin/Heidelberg, Germany: Springer International Publishing, 2022.
[10] Varshney, A., Kolhe, R., Gatne, S., Ingale, V. V: Arrhythmia Classification of ECG Signals Using Undecimated Discrete Wavelet Transform. In: 2022 IEEE 7th International conference for Convergence in Technology (I2CT). pp. 1–5 (2022). https://doi.org/10.1109/I2CT54291.2022.9824433.
[11] Bruna J.and Mallat S., "Invariant Scattering Convolution Networks," (2012), doi: https://doi.org/10.48550/.
[12] Lan, T., Zeng, Z., Han, L., Zeng, J.: Seismic Data Denoising Based on Wavelet Transform and the Residual Neural Network. Applied Sciences. 13, (2023). https://doi.org/10.3390/app13010655.
[13] Raji M.F. et al., A New Approach for Enhancing the Services of the 5G Mobile Network and IOT-Related Communication Devices Using Wavelet-OFDM and Its Applications in Healthcare, Sci. Program. 2020 (2020) 1–13, https://doi.org/ 10.1155/2020/3204695.
[14] Kustiyo A., Buono A., Faqih A., Priandana K., Analysis on Dimensionality Reduction Techniques for Sub-Seasonal to Seasonal Rainfall Prediction, in: in 2021 International Conference on Computer System, Information Technology, and Electrical Engineering (COSITE), (2021), pp. 156–160, https://doi.org/10.1109/ COSITE52651.2021.9649588.
[15] Gunasekaran, S., Rajan, S., Moses, L., Vikram, S., Subalakshmi, M., Shudhersini, B.: Wavelet Based CNN for Diagnosis of COVID 19 using Chest X Ray. IOP Conference Series: Materials Science and Engineering. 1084, 12015 (2021). https://doi.org/10.1088/1757-899X/1084/1/012015.
[16] Fernandes F.C.A., van Spaendonck R.L.C., Burrus C.S., A new framework for complex wavelet transforms, IEEE Trans. Signal Process. 51 (7) (2003) 1825–1837, https://doi.org/10.1109/TSP.2003.812841.
[17] Soro B., Lee, A Wavelet Scattering Feature Extraction Approach for Deep Neural Network Based Indoor Fingerprinting Localization, Sensors 19 (2019) 1790, https://doi.org/10.3390/s19081790.
[18] Tan, A., Wang, Y., Guo, T., Hou, X., Wang, S., Zhao, Y.: Quantitative analysis of multi-optical length NIR spectroscopy based on quaternion parallel feature extraction method. Infrared Physics & Technology. 119, 103964 (2021). https://doi.org/https://doi.org/10.1016/j.infrared.2021.103964.
[19] Chen, X., Zhou, J., Yuan, L., Huang, G., Chen, X., Shi, W.: Spectroscopic Identification of Environmental Microplastics. IEEE Access. PP, 1 (2021). https://doi.org/10.1109/ACCESS.2021.3063293.
[20] Back, H. de M., Vargas Junior, E.C., Alarcon, O.E., Pottmaier, D.: Training and evaluating machine learning algorithms for ocean microplastics classification through vibrational spectroscopy. Chemosphere. 287, 131903 (2022). https://doi.org/10.1016/j.chemosphere.2021.131903.
[21] Yan, X., Cao, Z., Murphy, A., Qiao, Y.: An Ensemble Machine Learning Method for Microplastics Identification with FTIR Spectrum. Journal of Environmental Chemical Engineering. 10, 108130 (2022). https://doi.org/10.1016/j.jece.2022.108130.
[22] Zhang L., Ding X., Hou R., Classification modeling method for near-infrared spectroscopy of tobacco based on multimodal convolution neural networks, J Anal Methods Chem. 2020 (2020) 1–13.
[23] McGill, C., Forsuelo, M., Guan, Y., Green, W.H.: Predicting Infrared Spectra with Message Passing Neural Networks. Journal of Chemical Information and Modeling. 61, 2594–2609 (2021). https://doi.org/10.1021/acs.jcim.1c00055.
[24] Chen, H., Chen, A., Xu, L., Xie, H., Qiao, H., Lin, Q., Cai, K.: A deep learning CNN architecture applied in smart near-infrared analysis of water pollution for agricultural irrigation resources. Agricultural Water Management. 240, 106303 (2020). https://doi.org/https://doi.org/10.1016/j.agwat.2020.106303.
[25] Jung H., Kim Y., Jang H., Ha N., Sohn K., Unsupervised deep image fusion with structure tensor representations, IEEE Trans Image Process. 29 (2020) 3845–3858, https://doi.org/10.1109/TIP.2020.2966075.
[26] Ailing Tan a , Yajie Zuo a , Yong Zhao b,* , Xiaohang Li a , Haijie Su a , Alan X. Wang, Qualitative analysis for microplastics based on GAF coding and IFCNN image fusion enabled FITR spectroscopy method, Infrared Physics and Technology, (2023).
[27] EL-Gammal, O.A., Alshater, H., El-Boraey, H.A.: Schiff base metal complexes of 4-methyl-1H-indol-3-carbaldehyde derivative as a series of potential antioxidants and antimicrobial: Synthesis, spectroscopic characterization and 3D molecular modeling. Journal of Molecular Structure. 1195, 220–230 (2019).
[28] Aly, S.A., Hassan, S.S., El-Boraey, H.A. et al. Synthesis, Biological Activity, and the Effect of Ionization Radiation on the Spectral, XRD, and TGA Analysis of Cu(I), Cu(II), Zn(II), and Cd(II) Complexes. Arab J Sci Eng (2023). https://doi.org/10.1007/s13369-023-07988-2.
[29] Aly, S.A.: Physico-chemical study of new ruthenium (III), Pd (II) and Co (II) complexes, DNA binding of Pd (II) complex and biological applications. Journal of Radiation Research and Applied Sciences. 11, 163–170 (2018).
[30] Aly, S.A., Elembaby, D.: Synthesis, spectroscopic characterization and study the effect of gamma irradiation on VO2+, Mn2+, Zn2+, Ru3+, Pd2+, Ag+ and Hg2+ complexes and antibacterial activities. Arabian Journal of Chemistry. 13, 4425–4447 (2020).
[31] Abdalla, E.M., Hassan, S.S., Elganzory, H.H., Aly, S.A., Alshater, H.: Molecular docking, dft calculations, effect of high energetic ionizing radiation, and biological evaluation of some novel metal (Ii) heteroleptic complexes bearing the thiosemicarbazone ligand. Molecules. 26, 5851 (2021).

[32] Aly, S.A., Hassan, S.S., Eldourghamy, A.S., Badr, E.E., El-Salamoney, M.A., Hassan, M.A., Elganzory, H.H.: Synthesis, characterization, XRD, SEM, DNA binding, and effect of γ-irradiation of some new Ni (II) and Co (II) complexes with thiosemicarbazone ligand: In vitro antimicrobial and antioxidant activities. Applied Organometallic Chemistry. 36, e6727 (2022).
[33] He, K., Zhang, X., Ren, S., Sun, J.: Deep residual learning for image recognition. Proceedings of the IEEE Computer Society Conference on Computer Vision and Pattern Recognition. 2016-Decem, 770–778 (2016). https://doi.org/10.1109/CVPR.2016.90.
[34] Gupta, A., Anjum, Gupta, S., Katarya, R.: InstaCovNet-19: A deep learning classification model for the detection of COVID-19 patients using Chest X-ray. Applied Soft Computing. 99, (2021). https://doi.org/10.1016/j.asoc.2020.106859.
[35] Ardakani, A.A., Kanafi, A.R., Acharya, U.R., Khadem, N., Mohammadi, A.: Application of deep learning technique to manage COVID-19 in routine clinical practice using CT images: Results of 10 convolutional neural networks. Computers in Biology and Medicine. 121, 103795 (2020). https://doi.org/10.1016/j.compbiomed.2020.103795.
[36] Nanni, L., Manfè, A., Maguolo, G., Lumini, A., Brahnam, S.: High performing ensemble of convolutional neural networks for insect pest image detection. Ecological Informatics. 67, (2022). https://doi.org/10.1016/j.ecoinf.2021.101515.
[37] Tan, M., Le, Q. V.: EfficientNet: Rethinking model scaling for convolutional neural networks. 36th International Conference on Machine Learning, ICML (2019), 10691–10700 (2019).
[38] Razali, N.F., Isa, I.S., Sulaiman, S.N., Noor, N.K., Osman, M.K.: CNN-Wavelet scattering textural feature fusion for classifying breast tissue in mammograms. Biomedical Signal Processing and Control. 83, 104683 (2023). https://doi.org/10.1016/j.bspc.2023.104683.
[39] Khemani, V., Azarian, M.H., Pecht, M.G.: Learnable Wavelet Scattering Networks: Applications to Fault Diagnosis of Analog Circuits and Rotating Machinery. Electronics (Switzerland). 11, (2022). https://doi.org/10.3390/electronics11030451.
[40] Renukadevi, T., Saraswathi, K., Prabu, P., Venkatachalam, K.: Brain image classification using time frequency extraction with histogram intensity similarity. Computer Systems Science and Engineering. 41, 645–660 (2022). https://doi.org/10.32604/csse.2022.020810.
[41] Kurniati, F.T., Manongga, D.H.F., Sediyono, E., Yulianto, S., Prasetya, J.: Object Classification Model Using Ensemble Learning with Gray- Level Co-Occurrence Matrix and Histogram Extraction. Jurnal Ilmiah Teknik Elektro Komputer dan Informatika (JITEKI). 9, 793–801 (2023). https://doi.org/10.26555/jiteki.v9i3.26683.
[42] Dash, S., Senapati, M.R.: Gray level run length matrix based on various illumination normalization techniques for texture classification. Evolutionary Intelligence. 14, 217–226 (2021). https://doi.org/10.1007/s12065-018-0164-2.
[43] Tang, Z., Zhang, H., Pun, C., Yu, M., Yu, C., Zhang, X.: Robust image hashing with visual attention model and invariant moments. https://doi.org/10.1049/iet-ipr.2019.1157.
[44] Zhu, T., Lin, Y., Liu, Y.: Synthetic minority oversampling technique for multiclass imbalance problems. Pattern Recognition. 72, 327–340 (2017). https://doi.org/10.1016/j.patcog.2017.07.024.
[45] Ogundokun, R.O., Maskeliunas, R., Misra, S., Damaševičius, R.: Improved CNN Based on Batch Normalization and Adam Optimizer. Lecture Notes in Computer Science (including subseries Lecture Notes in Artificial Intelligence and Lecture Notes in Bioinformatics). 13381 LNCS, 593–604 (2022). https://doi.org/10.1007/978-3-031-10548-7_43.
[46] Chuan T S, and Zhu S., "Binary search of the optimal cut-point value in ROC analysis using the F1 score." Journal of Physics: Conference Series. Vol. 2609. No. 1. IOP Publishing, 2023.
[47] Lu, F., Liu, G.H.: Image retrieval using contrastive weight aggregation histograms. Digital Signal Processing: A Review Journal. 123, 103457 (2022). https://doi.org/10.1016/j.dsp.2022.103457.
[48] Zhang, H., Wang, P., Gao, X., Qi, Y., Gao, H.: Out-of-sample data visualization using bi-kernel t-SNE. Information Visualization. 20, 20–34 (2021). https://doi.org/10.1177/1473871620978209.

Authors' Profiles

Dr. Asmaa S. Abdo is an Assistant Professor in the Information Systems Department at the Faculty of Computers and Artificial Intelligence, University of Sadat City, Egypt. She works as the deputy director of the Electronic Tests Unit, University of Sadat City. Dr. Asmaa received her B.Sc. degree in 2011, M.Sc. degree in 2016, and Ph.D. in 2022 from the Information Systems Department at the Faculty of Computers and Information, Menoufia University. She is a member at Scientific Research School of Egypt (SRSEG). Also, she was invited as a reviewer from many international conferences and journals. Dr. Asmaa research interests include Data Mining, Information systems, Data Quality, and Artificial Intelligence.

Dr. Kamel K. Mohammed is an accomplished BioMed engineering researcher specializing in ultrasound imaging, AI, and medical innovation. Kamel holds a PhD in Biomedical Engineering and Systems from Cairo University, he developed an objective evaluation method for ultrasound images, enhancing image quality and disease detection. Published in renowned journals, his work includes AI applications for COVID-19. He excels in medical imaging and is an active participant in innovation programs, securing 2nd place in Siemens Healthineers' Think Tank Certification Program. His interdisciplinary work contributes to novel healthcare solutions, exploring metaverse technology. Well-regarded in his field, he continuously pushes the boundaries of biomedical research, aiming to improve healthcare outcomes with AI integration. Kamel's research interests include developing AI systems for automated analysis of medical images and bio signals. His current work focuses on applying deep learning for lung cancer detection in CT scans. He also has experience in designing wearable sensors for mobile health applications. He has co-authored over 18 publications and serves as member in scientific research school of Egypt (SRSEG).

Dr. Rania Ahmed, Assistant professor at the faculty of Computers and Artificial Intelligence in Modern University for Technology and Information. Dr. Rania Ahmed is Lecturer science 2017; she got her PhD from the Menoufia University in Egypt in 2017 in Computer Science. In the field of Artificial Intelligence. She received the Bachelor in Computer Science degree from the Helwan University in 2006 and the Master in Computer Science degree from the Helwan University in 2010. In 2008 she worked as a Teacher in Faculty of Computers and Artificial Intelligence, Modern University. Dr. Rania has academic publications which include papers in international journals and conference proceedings. Her publications have appeared in international journals, conferences, and publishing houses such as Springer and Science Direct (Elsevier). Currently, Dr Rania is a member of the Scientific Research School of Egypt (SRSEG).

Dr. Heba Alshater. is a member of Scientific Research School of Egypt (SRSEG) and Associated Professor at Menoufia University Hospital at Forensic Medicine and Clinical Toxicology Department. Dr. Heba worked in Saudi Arabia in King Abdelaziz and Jeddah University, Faculty of Arts and Science for five years as assistant professor in chemistry department. Dr. Heba touched courses for students of postgrad in Faculty of Science and Faculty of Medicine Forensic Medicine and Clinical Toxicology Department in Menoufia University Hospital till now. Responsible of laboratory of Forensic Medicine and Clinical Toxicology Department in University Hospital. Dr. Heba won awards including the Best Researcher of Publishing at Faculty of Medicine for two years. Dr. Heba is interested in nanotechnology, synthesis and characterization of nanoparticles and Schiff base metal complexes. Dr. Heba have several publications in springer and Elsevier.

Prof. Samar A. Aly is professor doctor at Genetic Engineering and Biotechnology Research Institute, University of Sadat City, Department of Environmental Biotechnology. Prof.Dr. Samar worked in Saudi Arabia in Qassim University, Buraidah, Faculty of art and science for three years in chemistry department. Prof.Dr. Samar won awards including the best researcher of publishing of University of Sadat City 2022. Area of interesting of. Prof.dr samar is bioinorganic chemistry included synthesis, characterization of metal complexes and biological application; Study the effect of gamma irradiation on new metal complexes and antitumor activity; Biological screening of some nano mono and binuclear metal complexes of new hydrazone ligand.

Prof. Ashraf Darwish is a Professor of Computer Science and former Acting Head of the Mathematics and Computer Science Department at the Faculty of Science, Helwan University, Egypt. He earned his Ph.D. in computer science from Saint Petersburg State University, Russian Federation, in 2006. Professor Darwish is the Vice Chair of the Scientific Research School in Egypt (SRSEG), formerly called Scientific Research Group in Egypt (SRGE), in Computer Science and Information Technology. Professor Ashraf Darwish is a distinguished Professor with a focus on advancing Artificial Intelligence (AI) and its applications, specializing in areas such as machine learning, deep learning, and computer vision. His expertise extends to cutting-edge technologies like Digital Twins, the emerging field of the Metaverse, Explainable Artificial Intelligence, and Generative Artificial Intelligence. With a rich academic background, Professor Darwish serves as the editor-in-chief and associate editor for several prestigious international journals, and he holds senior membership in various computing international associations, including IEEE. His extensive academic journey is marked by numerous contributions, encompassing papers, books, and book chapters published in reputable international journals and conference proceedings. From 2011 to 2015, Professor Darwish represented Egypt in diplomatic affairs as the Cultural and Educational Chancellor to the Republic of Kazakhstan and Central Asia. Acknowledging his outstanding contributions, Professor Darwish was honored with the Best Researcher award in 2014 at Helwan University, Egypt. Notably, he is recognized among the top 2% of top-cited scientists in Artificial Intelligence & Image Processing, as well as subfields of Fluids & Plasmas and Information & Communication Technologies, based on Stanford University's Ioannidis's index published in 2022 and 2023. Currently, Professor Darwish holds the esteemed position of Chancellor at the Egyptian Chinese University in Cairo. Additionally, he is a Member of the Council of Communication Research and Information Technology at ASRT, Ministry of Higher Education and Scientific Research of Egypt.

Prof. Aboul Ella Hassanein is the Founder and Head of the Egyptian Scientific Research School of Egypt (SRSEG) and a Professor of Information Technology at the Faculty of Computer and Information, Cairo University. Professor Hassanien is ex-dean of the faculty of computers and information, Beni Suef University. Professor Hassanien has more than 800 scientific research papers published in prestigious international journals and over 40 books covering such diverse topics as data mining, medical images, intelligent systems, social networks and smart environment. Prof. Hassanien won several awards including the Best Researcher of the Youth Award of Astronomy and Geophysics of the National Research Institute, Academy of Scientific Research (Egypt, 1990). He was also granted a scientific excellence award in humanities from the University of Kuwait for the 2004 Award and received the superiority of scientific - University Award (Cairo University, 2013). Also, he honored in Egypt as the best researcher in Cairo University in 2013. He was also received the Islamic Educational, Scientific and Cultural Organization (ISESCO) prize on Technology (2014) and received the state Award for excellence in engineering sciences 2015. He was awarded the medal of Sciences and Arts of the first class by the President of the Arab Republic of Egypt, 2017.

How to cite this paper: Asmaa S. Abdo, Kamel K. Mohammed, Rania Ahmed, Heba Alshater, Samar A. Aly, Ashraf Darwish, Aboul Ella Hassanein, "Infrared Images Spectra Multi-class Classification Model Based on Deep Learning", International Journal of Intelligent Systems and Applications(IJISA), Vol.16, No.4, pp.22-38, 2024. DOI:10.5815/ijisa.2024.04.02